

Supporting information

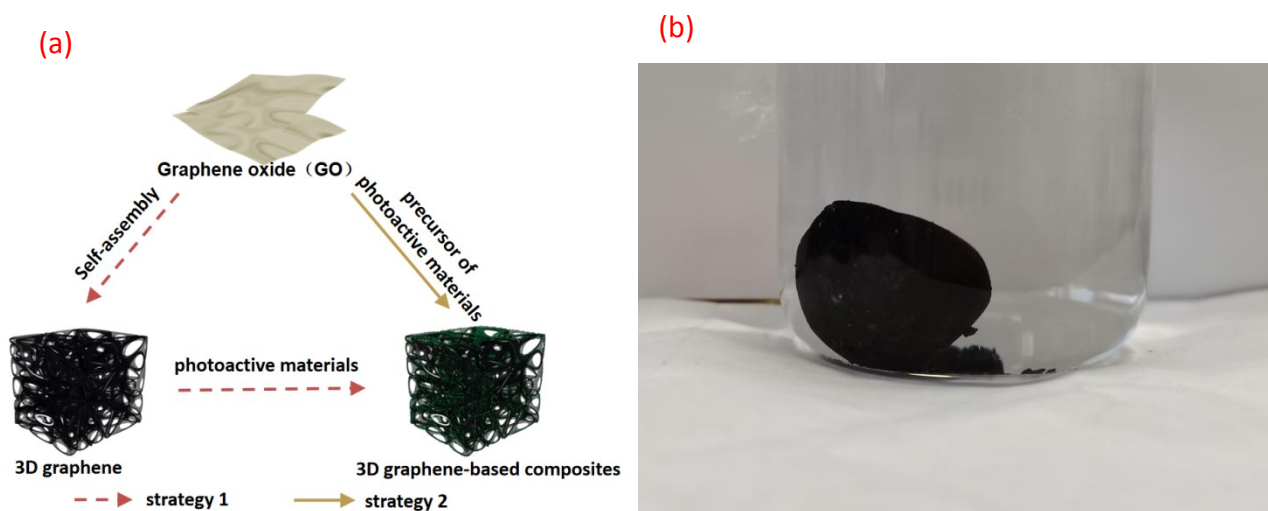


Figure S1. (a) Two strategies for graphene oxide synthesis of 3D graphene-based composites; (b) photograph of CuI-BiOI/rGO hydrogel

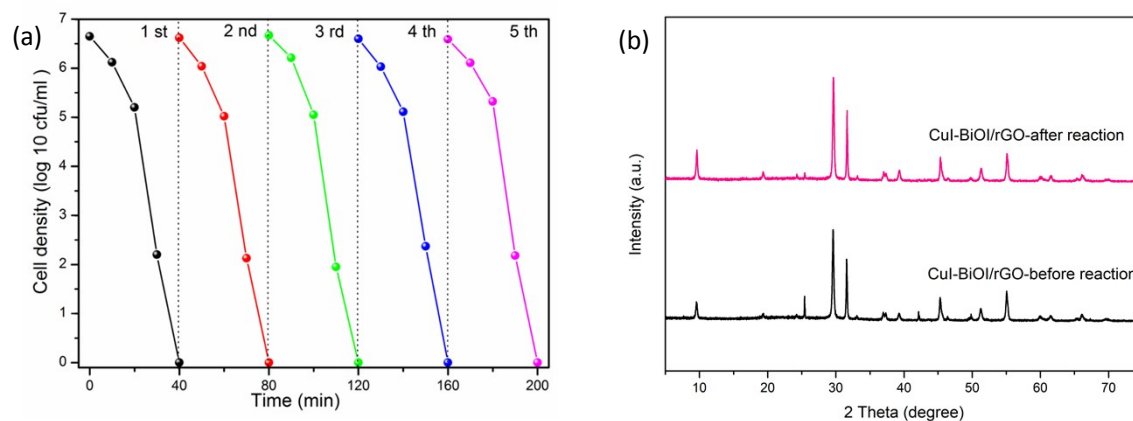


Figure S2. (a) Five cycling experiment in the disinfection performance with CuI-BiOI/rGO hydrogel under visible light irradiation and (b) XRD spectra before and after antibacterial reaction of CuI-BiOI/rGO hydrogel

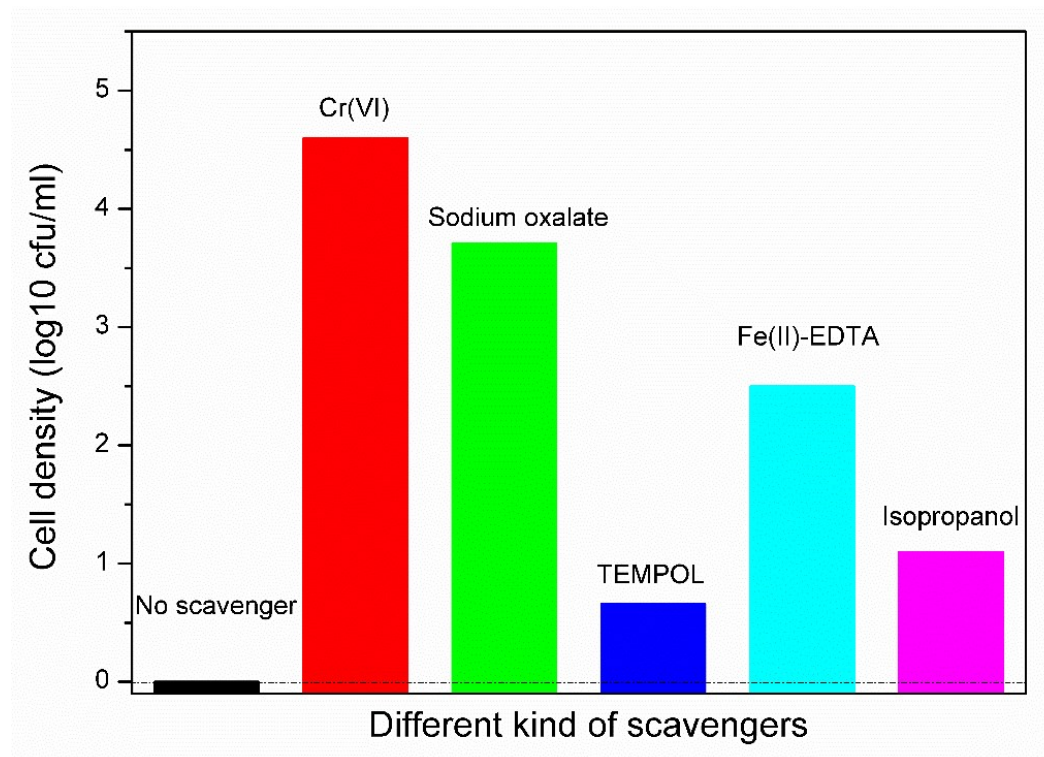


Figure. S3. Photocatalytic inactivation efficiency against *E. coli* K-12 ($10^{6.5}$ cfu/mL) with different scavengers (0.5 mM sodium oxalate, 0.5 mM isopropanol, 0.05 mM Cr(VI), 2 mM TEMPOL and 0.1 mM Fe(II)–EDTA) in the presence of CuI–BiOI/rGO hydrogel under visible light irradiation.

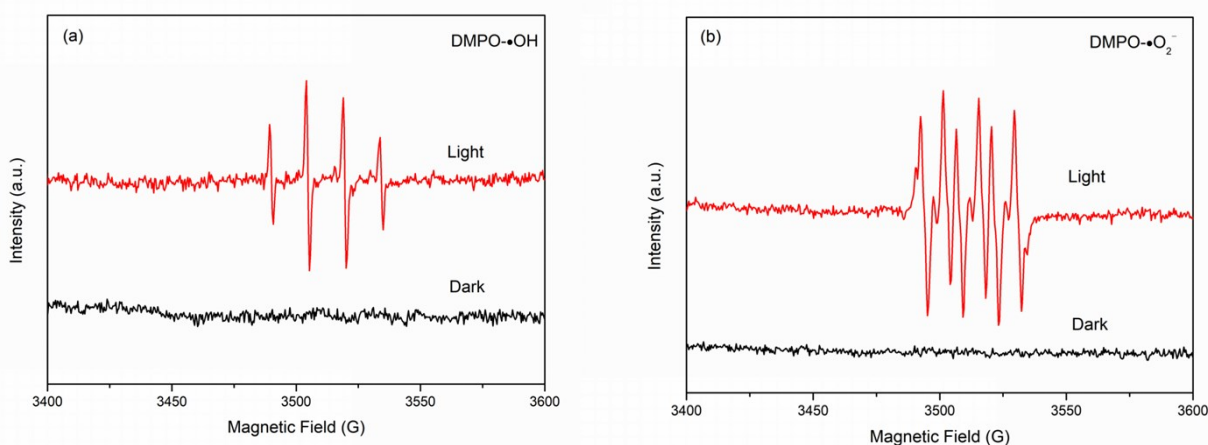


Figure S4. ESR spectra of: (a) DMPO-•OH adducts in aqueous suspension and (b) DMPO-•O₂⁻ adducts in methanol suspension under visible irradiation and dark conditions in CuI–BiOI/rGO hydrogel

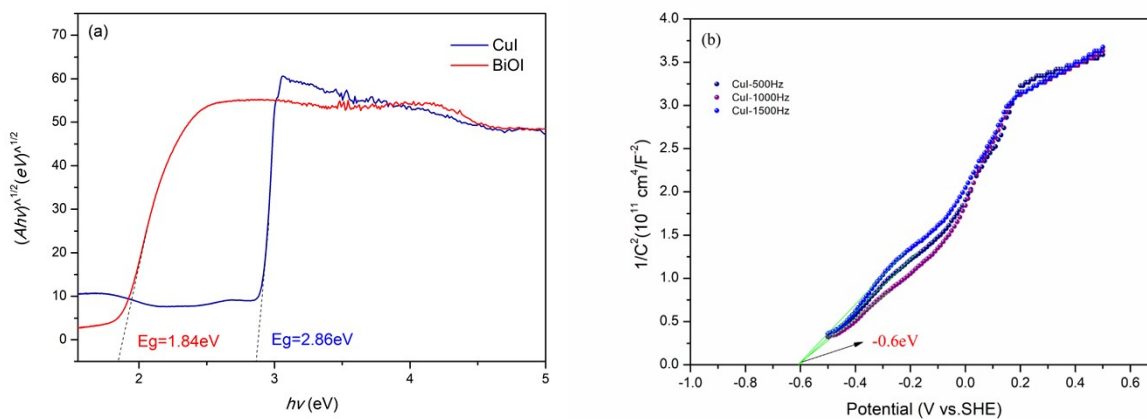


Figure S5. (a) Band gap energy spectra of CuI and BiOI and (b) Mott Schottky curve of CuI

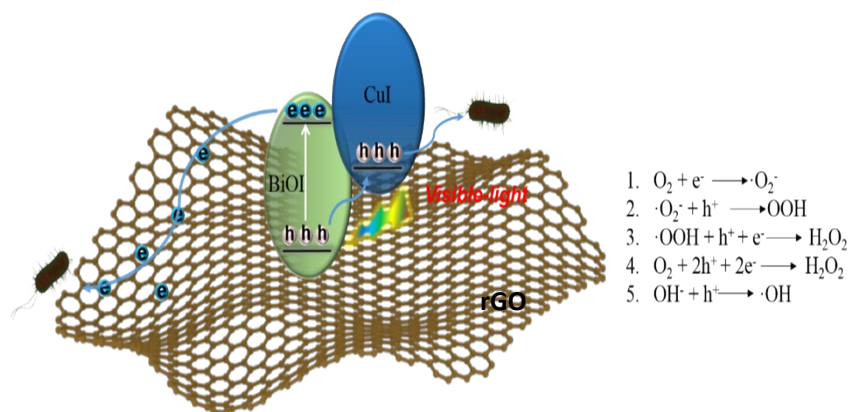


Figure S6. Schematic drawing of the photocatalytic antibacterial process of CuI-BiOI/rGO hydrogel